Defining Stem Cell Dynamics in Models of Intestinal Tumor Initiation

Louis Vermeulen *et al.*

Science **342**, 995 (2013);
DOI: 10.1126/science.1243148

Science (print ISSN 0036-8075; online ISSN 1095-9203) is published weekly, except the last week in December, by the American Association for the Advancement of Science, 1200 New York Avenue NW, Washington, DC 20005.

48. E. W. Miller, O. Tulyathan, E. Y. Isacoff, C. J. Chang, *Nat. Chem. Biol.* **3**, 263–267 (2007).
49. E. A. Veal, A. M. Day, B. A. Morgan, *Mol. Cell* **26**, 1–14 (2007).

Acknowledgments: This work was supported by grants from the NIH (GM 040541 to H.-w.L. and GM 069657 to C.K. and J.M.B.), the Welch Foundation (F-1511 to H.-w.L.), and the NSF (MCB-0642058 to C.K. and J.M.B.). We thank M. T. Green for helpful discussions.

Supplementary Materials
www.sciencemag.org/content/342/6161/991/suppl/DC1
Materials and Methods
Figs. S1 to S7
References (*50*–*67*)

10 May 2013; accepted 1 October 2013
Published online 10 October 2013;
10.1126/science.1240373

Defining Stem Cell Dynamics in Models of Intestinal Tumor Initiation

Louis Vermeulen,[1,2]*† Edward Morrissey,[1]* Maartje van der Heijden,[1,2] Anna M. Nicholson,[1] Andrea Sottoriva,[3] Simon Buczacki,[1] Richard Kemp,[1] Simon Tavaré,[1,4] Douglas J. Winton[1]

Cancer is a disease in which cells accumulate genetic aberrations that are believed to confer a clonal advantage over cells in the surrounding tissue. However, the quantitative benefit of frequently occurring mutations during tumor development remains unknown. We quantified the competitive advantage of *Apc* loss, *Kras* activation, and *P53* mutations in the mouse intestine. Our findings indicate that the fate conferred by these mutations is not deterministic, and many mutated stem cells are replaced by wild-type stem cells after biased, but still stochastic events. Furthermore, *P53* mutations display a condition-dependent advantage, and especially in colitis-affected intestines, clones harboring mutations in this gene are favored. Our work confirms the previously theoretical notion that the tissue architecture of the intestine suppresses the accumulation of mutated lineages.

Cancer development involves competition between normal and deviant cell lineages, ultimately resulting in disruptive tissue overgrowth (*1*). The cellular effects of mutations can increase proliferation or impair response to cell death–inducing signals (*2*). However, only very limited quantitative data exist on the net effects of oncogenic alterations at the cell population level. In the intestine, cancer arises from an initial transformation event occurring primarily, but not exclusively, in the stem cell compartment (*3*, *4*). Because normal intestinal crypt homeostasis is characterized by competition between equipotent stem cells that continuously replace each other in a random fashion (Fig. 1A) (*5*, *6*), oncogenic mutations may confer an advantage on the clone in which they arise by acting on these dynamics. We confirmed and used this assumption to quantify the competitive benefit of mutations frequently occurring in colorectal cancer (CRC).

To track the fate of wild-type (WT) and mutated cell lineages, we induced low-level intestinal recombination either specifically in the crypt base using *Lgr5*-EGFP-Cre^{ER} mice or more generally in *Ah*Cre^{ER} mice, both crossed to the R26-Lox-STOP-Lox-*tdTomato* (tdTom$^{fl/fl}$) reporter strain. Clones were visualized and quantified at the bottom of the crypt, allowing robust clone size quantification around the circumference of the crypt (fig. S1). We observed that on average, clones expand, and the number of fixed clones (i.e., crypts within which the whole epithelium is tdTom^{+}) increases with time (Fig. 1, B to E). By quantitative analysis of the clone size distributions using the stochastic master equation and Bayesian inference, we confirmed earlier studies that continuous, one-dimensional neutral replacements govern intestinal stem cell dynamics (figs. S2 and S3) (*5*, *6*). This process is fully defined by only two parameters: the number of functional stem cells per crypt (N) and the rate at which these replace each other (λ). Because of the high-quality clone size distribution data we obtained, we can directly infer both N and λ with considerable precision (fig. S2). For the proximal small intestine (SI), we find that $N = 5$ and $\lambda = 0.1$ replacements per stem cell per day (figs. S2 and S3). This inferred number of stem cells is considerably lower than the number of Lgr5^{+} cells (~16) per crypt (*5*) but agrees with a functional marker-free estimate of stem cell numbers (*7*). In fact, we directly confirmed a previous suggestion that a sizable fraction of Lgr5^{+} cells are actually more committed progenitor cells and do not function as stem cells in homeostasis (*8*) (fig. S4).

Next, we crossed *Ah*Cre^{ER}/tdTom^{-fl} mice with *Kras*-G12D^{fl} and *Apc*$^{fl/fl}$ mice. Recombination in these mice will result in activation of an oncogenic *Kras* variant or inactivation of one or both copies of the negative Wnt regulator *Apc*, in addition to tdTom expression. We confirmed that tdTom expression is tightly matched to oncogenic recombination events (fig. S5). Furthermore, our analysis was facilitated by the fact that the low-level clone induction of pre-neoplastic lineages does not substantially alter tissue morphology, as has been reported before (*9*, *10*) (Fig. 1B and fig. S6). We found that activated KRAS confers an evident clonal advantage as the *Kras*^{G12D} harboring clones expand and become fixed more rapidly than the WT lineages (Fig. 1, B to E). In order to express this effect quantitatively, we introduced an additional variable to the one-dimensional drift model to capture the biased drift properties: P_R signifies the chance that a tdTom^{+} stem cell replaces its nonlabeled neighbor; conversely, 1-P_R represents the chance that the nonlabeled stem cell replaces the tdTom^{+} neighboring stem cell. The neutral version of the model is described by unbiased stochastic replacements, and as expected, using the inference method in combination with the neutral clone size distribution data we find P_R(WT versus WT) = 0.50 [0.48 to 0.52, 95% confidence interval (CI)] (Fig. 1F), indicating that two adjacent stem cells have equal probability to replace each other. Applying this inference strategy to the biased drift data of *Kras* mutant clones, we found a well-demarcated posterior probability peak: P_R(*Kras*^{G12D} versus WT) = 0.78 (0.75 to 0.81, 95% CI) (Fig. 1G). This implies that for replacement events occurring at the interface of a *Kras*^{G12D} and a WT clone, the *Kras* mutant stem cell replaces the WT stem cell in ~80% of the cases, and conversely that the WT stem cell replaces the mutant stem cell in ~20% of the replacement events. Thus, interpreting the altered size distribution of clones in terms of individual stem cell fates provides an intuitive estimate of the potency of oncogenic mutations in the context of a stochastic model, by integrating the effects of proliferation rate, cell death frequencies, and self-renewal properties into a single parameter (P_R).

Because human CRCs arise in the majority of cases after the inactivation of *APC*, we determined the clonal advantage of lineages harboring either heterozygous or homozygous inactivating mutations within this gene. *Apc*$^{+/-}$ lineages display only a limited, but significant, benefit over WT clones, whereas *Apc*$^{-/-}$ lineages have a more marked clonal benefit already at 4 days, making it unlikely that secondary effects of *Apc* loss [such as chromosomal instability (CIN)] are involved (Fig. 2, A to C). After applying the inference strategy to this data to determine P_R, we found that P_R(*Apc*$^{+/-}$ versus WT) = 0.62 (0.58 to 0.66, 95% CI) and P_R(*Apc*$^{-/-}$ versus WT) = 0.79 (0.75 to 0.82, 95% CI) (Fig. 2, D and E). In reality, *Apc*$^{-/-}$

[1]Cancer Research UK, Cambridge Institute, University of Cambridge, Robinson Way, Cambridge CB2 ORE, UK. [2]Laboratory for Experimental Oncology and Radiobiology, Center for Experimental Molecular Medicine, Academic Medical Center, Meibergdreef 9, 1105 AZ, Amsterdam, Netherlands. [3]Department of Preventive Medicine, Keck School of Medicine, University of Southern California, Los Angeles, CA, USA. [4]Department of Biological Sciences, University of Southern California, Los Angeles, CA, USA.

*These authors contributed equally to this work.
†Corresponding author. E-mail: l.vermeulen@amc.uva.nl

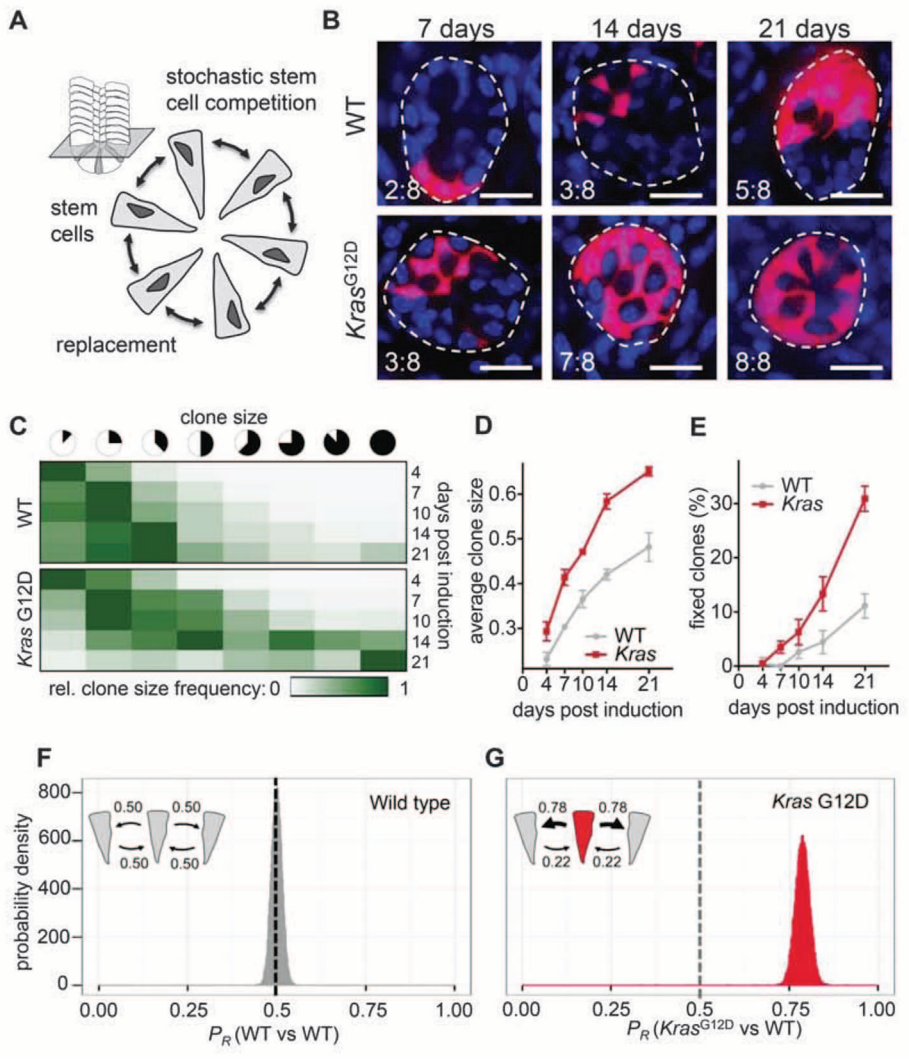

Fig. 1. Quantifying the clonal benefit of *Kras*^{G12D}. (**A**) Intestinal stem cells are equipotent and continuously replace each other in a stochastic fashion. (**B**) Confocal images of SI crypt bottoms of *Ah*Cre^{ER}/tdTom$^{-/fl}$ mice (WT) and *Ah*Cre^{ER}/tdTom$^{-/fl}$/*Kras*-G12D^{fl} (*Kras*^{G12D}) at the indicated time points after clone induction. Clone sizes are indicated as fractions (in eighths) of the crypt circumference. Blue, nuclear stain (DAPI); red, tdTom expression; scale bars represent 30 μm. (**C**) Heat maps depict the relative frequency of clones of the indicated size (columns) at various time points (rows) for both WT and *Kras*^{G12D}. (**D** and **E**) Graph displays the average size (D) or the percentage of fixed clones (E) of WT and *Kras*^{G12D} clones at different time points after induction. Error bars indicate the SEM. [(C) to (E)] $N = 5$ mice for each group; for each time point and condition, >200 clones were analyzed. (**F** and **G**) Bayesian inference of the biased drift parameter P_R for WT versus WT (F) and *Kras*^{G12D} versus WT (G) clones. The vertical axis indicates the probability density; the horizontal axis indicates the P_R values. The higher the probability density value, the more likely this P_R value underlies the observed biased drift. $P_R = 0.5$ indicates neutral drift. The cartoons summarize the replacement properties (with color coding as in the graphs).

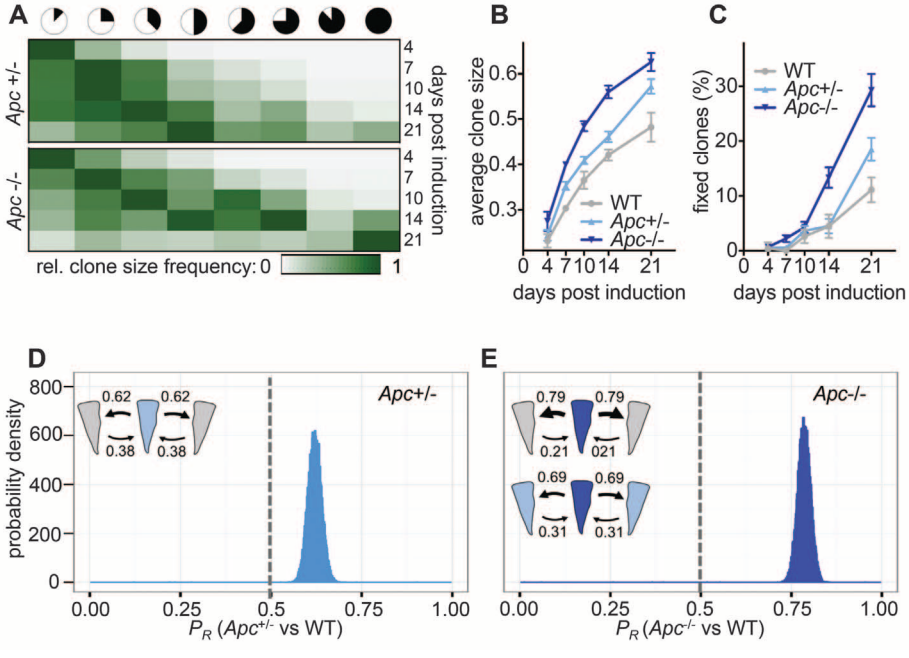

Fig. 2. Quantifying the clonal benefit of *Apc* loss. (**A**) Heat maps depict the relative frequency of clones of the indicated size (columns) at various time points (rows) for *Apc*$^{+/-}$ and *Apc*$^{-/-}$. (**B** and **C**) Graph displays the average size (B) or the percentage of fixed clones (C) of WT, *Apc*$^{+/-}$, and *Apc*$^{-/-}$ clones at different time points after induction. Error bars indicate the SEM. WT is as in Fig. 1. [(A) to (C)] $N = 5$ mice for each group; for each time point and condition, >200 clones were analyzed. (**D** and **E**) Bayesian inference of the biased drift parameter P_R for *Apc*$^{+/-}$ versus WT (D) and *Apc*$^{-/-}$ versus WT (E).

mutations usually occur in a clone of $Apc^{+/-}$ cells because of loss of heterozygosity (LOH) or an independent additional mutation (*10*); therefore, we also calculated the benefit of $Apc^{-/-}$ stem cells over $Apc^{+/-}$ stem cells: $P_R(Apc^{-/-}$ versus $Apc^{+/-}) = 0.69$ (0.65 to 0.72, 95% CI) (Fig. 2E). Both in the case of $Kras^{G12D}$ and in the case of the inactivation of *Apc*, the inferred values for P_R result in clone size distributions in accordance with the measured data (fig. S7). A further confirmation of the validity of the model comes from the observation that $tdTom^+$ clones induced in Apc^{Min} mice, which are characterized by a heterozygous germline *Apc* mutation, display similar dynamics to neutral clones in a WT background [$P_R(Apc^{Min}$ versus $Apc^{Min}) = 0.48$ (0.46 to 0.51, 95% CI)], indicating neutral competition between $Apc^{+/-}$ lineages, although clones holding this mutation clearly have an advantage over WT clones (fig. S8).

Our findings reveal that although $Kras^{G12D}$ mutations or the inactivation of *Apc* result in a marked competitive advantage of the respective cell lineage, this does not mean that the clone will become deterministically fixed. Mutated stem cells are commonly replaced by WT stem cells, thereby evading the accumulation of further mutations. By using the inferred parameters of the biased drift model (N, λ, P_R) and the adapted stochastic master equations, we calculated the proportion of mutant clones that reach fixation at a particular clone age (Fig. 3A). This analysis reveals that the majority of stem cells acquiring an $Apc^{+/-}$ mutation will be stochastically replaced by WT stem cells, and these mutant lineages will disappear from the tissue. In addition only ~55% of $Apc^{-/-}$ mutant stem cells within an $Apc^{+/-}$ background will reach fixation. These findings reveal that the accumulation of mutations in the intestinal tissue is an inefficient process because of the particular tissue architecture and the continuous stochastic replacements of stem cells. To illustrate the inefficiency of the process, we determined the contribution of different mutational trajectories in the formation of aberrant crypt foci (ACF); i.e., a crypt with a fixed $Apc^{-/-}$ clone (Fig. 3B). Only 22% of the ACFs result from two subsequent *Apc* hits (or LOH), and a large proportion of ACFs arise in crypts in which multiple *Apc* hits have

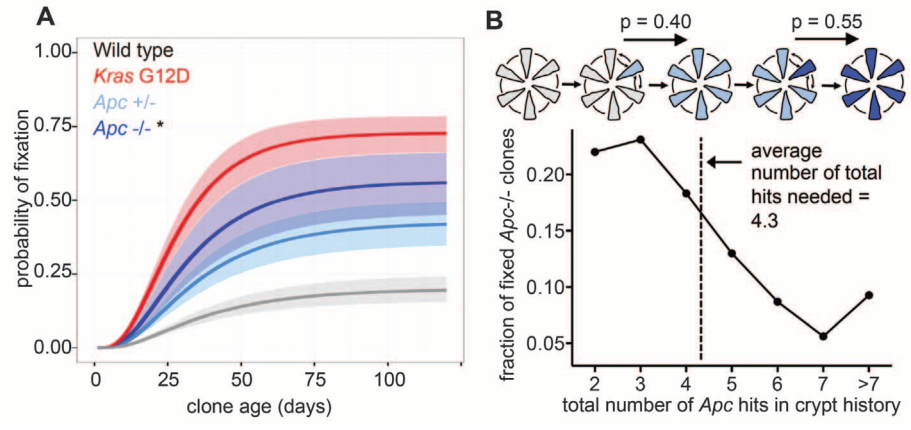

Fig. 3. Mutational trajectories. (**A**) Graph depicts the likelihood of the indicated clone types reaching fixation in a crypt over time. Shaded areas indicate 95% CI. (**B**) Cartoon summarizes the most direct way to reach the stage of a fixed $Apc^{-/-}$ clone. The fixation probabilities are indicated in the figure [value at 100 days in (A)]. The graph depicts the proportion of fixed $Apc^{-/-}$ clones (vertical axis) that arise after the total number of *Apc* hits, indicated at the horizontal axis.

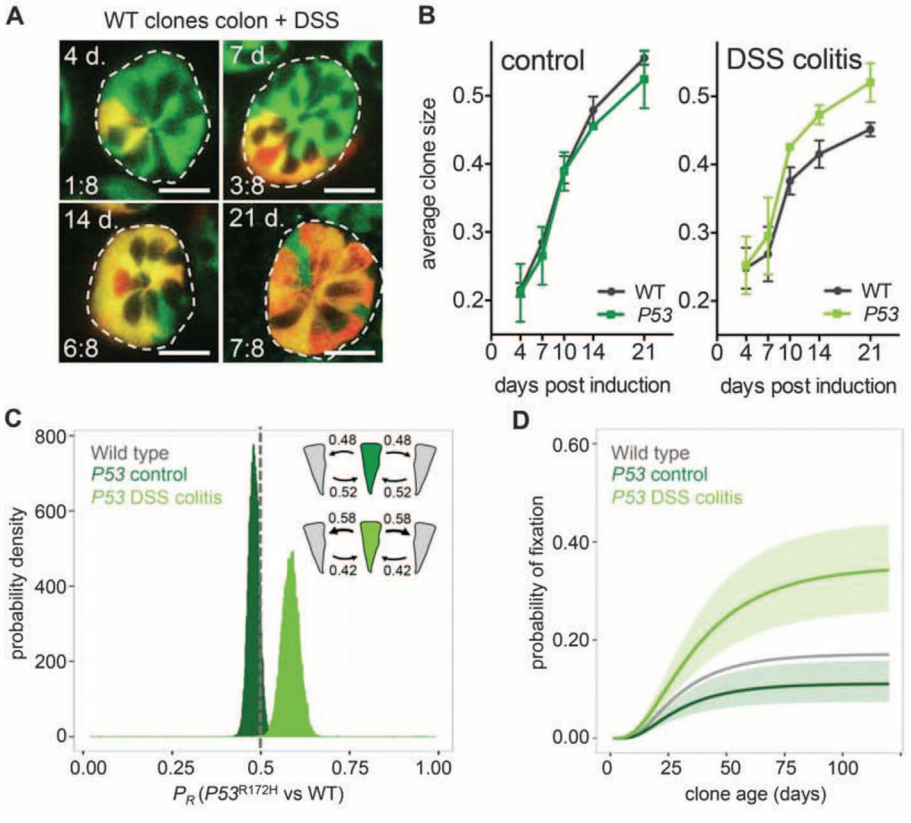

Fig. 4. *P53* mutations confer a condition-dependent clonal advantage. (**A**) Confocal images of colonic crypt bottoms of DSS-treated *Lgr5*-Cre^{ER}/$tdTom^{-/fl}$ mice at the indicated time points after clone induction. Clone sizes are indicated in eighths of the crypt circumference. Green, *Lgr5*-GFP; red, tdTom; scale bars represent 30 μm. (**B**) Graph depicts the average size of WT or $P53^{R172H}$ clones at different time points after induction in a control (left) and colitis (right) setting. Error bars indicate the SEM, $N = 5$ mice for each group; for each time point and condition, >150 clones were analyzed. (**C**) Bayesian inference of the biased drift parameter P_R for $P53^{R172H}$ versus WT in control animals and DSS-treated animals (colitis). (**D**) Graph depicts the likelihood of $P53^{R172H}$ clones to reach fixation in homeostasis and in colitis. Shaded areas indicate 95% CI.

taken place, the majority of which have been eliminated through the stochastic loss of mutant stem cells (Fig. 3B and fig. S9). Incorporating the inefficiency of fixation of the earliest events in CRC into a simple model describing the population incidence of this disease (*11*) highlights how these values could be used in future studies to link them to cancer frequencies in the human population (fig. S9).

Because *TP53* mutations are often seen in patients with CRC (*2*), we next investigated the effect of the dominant-negative hotspot mutation $P53^{R172H}$. However, no significant benefit of this mutation could be detected in the SI (fig. S8). Because *TP53* is reported to be of particular importance in colitis-associated CRC formation (*12*), we also studied *P53* mutations in a chronic colitis model (Fig. 4). Colitis was induced by feeding mice dextran sodium sulfate (DSS) starting a week before clone induction and was maintained until analysis of clone size distributions (Fig. 4, A and B, and fig. S10). Colitis induces a shift in stem cell dynamics in the colon, mainly by reducing the replacement rate (fig. S2), and although $P53^{R172H}$ did not confer a benefit to colon stem cells under normal conditions, in colitis, it significantly increases fitness: P_R ($P53^{R172H}$ versus WT) = 0.48 (0.45 to 0.51, 95% CI) and P_R^{colits}($P53^{R172H}$ versus WT) = 0.58, (0.54 to 0.63, 95% CI), respectively (Fig. 4C). Therefore, *P53* mutated clones have an increased likelihood to become fixed in a gut affected by inflammation (Fig. 4D). This presumably reflects the benefit of *P53*-mutated cells in dealing with colitis-associated reactive oxygen species formation (*13*). More generally, this result demonstrates that the competitive benefit of mutations during tumor initiation is dependent on the context in which they arise.

Our work presents a quantification of the effects of relevant mutations on stem cell dynamics during the initiation of a solid malignancy. A limited competitive advantage of common mutations in CRC is revealed, and many mutations that occur are lost from the population because of stochastic, albeit biased, replacement by neighboring WT lineages. This finding supports the accepted but so far theoretical notion that the tissue architecture and the features of the "evolutionary graph" representing the intestinal stem cell population prevent deterministic fixation of mutated lineages (*14*–*16*). The values now placed on the clonal advantages conferred by common mutations can be used in future modeling studies of tumor initiation in the intestine that so far have not used experimentally derived values for the benefits of individual mutations (*17*). This will help to assess other phenomena associated with CRC development, such as CIN (*18*). Furthermore, our work reveals that the potential competitive benefits of mutations are dependent on the environment in which they arise and provides a compelling explanation of why *TP53* mutations are found frequently and already at early stages in colitis-associated CRC (*12*). The method used here provides a powerful tool to investigate therapeutic strategies to specifically eradicate (pre-) neoplastic stem cells while preserving their normal counterparts.

References and Notes

1. P. C. Nowell, *Science* **194**, 23–28 (1976).
2. E. R. Fearon, B. Vogelstein, *Cell* **61**, 759–767 (1990).
3. N. Barker *et al.*, *Nature* **457**, 608–611 (2009).
4. S. Schwitalla *et al.*, *Cell* **152**, 25–38 (2013).
5. H. J. Snippert *et al.*, *Cell* **143**, 134–144 (2010).
6. C. Lopez-Garcia, A. M. Klein, B. D. Simons, D. J. Winton, *Science* **330**, 822–825 (2010).
7. S. Kozar *et al.*, *Cell Stem Cell* **13**, 626–633 (2013).
8. S. J. Buczacki *et al.*, *Nature* **495**, 65–69 (2013).
9. O. J. Sansom *et al.*, *Proc. Natl. Acad. Sci. U.S.A.* **103**, 14122–14127 (2006).
10. J. M. Fischer, A. J. Miller, D. Shibata, R. M. Liskay, *Oncogene* **31**, 2028–2038 (2012).
11. P. Calabrese, S. Tavaré, D. Shibata, *Am. J. Pathol.* **164**, 1337–1346 (2004).
12. S. J. Leedham *et al.*, *Gastroenterology* **136**, 542, e6 (2009).
13. L. B. Meira *et al.*, *J. Clin. Invest.* **118**, 2516–2525 (2008).
14. M. A. Nowak, F. Michor, Y. Iwasa, *Proc. Natl. Acad. Sci. U.S.A.* **100**, 14966–14969 (2003).
15. F. Michor, Y. Iwasa, H. Rajagopalan, C. Lengauer, M. A. Nowak, *Cell Cycle* **3**, 358–362 (2004).
16. E. Lieberman, C. Hauert, M. A. Nowak, *Nature* **433**, 312–316 (2005).
17. I. Bozic *et al.*, *Proc. Natl. Acad. Sci. U.S.A.* **107**, 18545–18550 (2010).
18. M. A. Nowak *et al.*, *Proc. Natl. Acad. Sci. U.S.A.* **99**, 16226–16231 (2002).

Acknowledgments: We thank the Cambridge Institute Biological Resource Unit for animal husbandry and F. De Sousa E Melo, J. P. Medema, and P. Calabrese for useful discussion. This work was supported by Cancer Research UK; L.V. received a fellowship from the Koningin Wilhelmina Fonds (KWF, Dutch Cancer Society). We declare no competing financial interests.

Supplementary Materials

www.sciencemag.org/content/342/6161/995/suppl/DC1
Materials and Methods
Figs. S1 to S10
References (*19*–*40*)

12 July 2013; accepted 22 October 2013
10.1126/science.1243148

Unwanted Evolution

Ivana Bozic and Martin A. Nowak

Science **342**, 938 (2013);
DOI: 10.1126/science.1247887

Science (print ISSN 0036-8075; online ISSN 1095-9203) is published weekly, except the last week in December, by the American Association for the Advancement of Science, 1200 New York Avenue NW, Washington, DC 20005.

CANCER

Unwanted Evolution

The dynamics of stem cell replacement at the bottom of the intestinal crypt is visualized and quantified.

Ivana Bozic[1,2] and Martin A. Nowak[1,2,3]

We mostly think of evolution as a process that has the power to build structures of incredible beauty and functionality, like multicellular organisms, the nervous system, and human language. But evolutionary dynamics can also lead to processes that are not wanted, such as cancer, because they oppose the survival interests of the organism. The somatic evolution of cancer is a consequence of our cells being individual replicators. Upon acquiring mutations, cells can revert to their primitive program of proliferation, competition for survival, and selection of the fittest. On page 995 of this issue, Vermeulen *et al*. (*1*) demonstrate how multicellular organisms keep this unwanted evolution in check. By quantifying the effects of mutations that frequently occur during colorectal tumor development, the authors show that intestinal tissue architecture acts as a suppressor of selection.

One way to prevent unwanted evolution is to hold somatic mutation rates low. The mutation rate in healthy human cells is on the order of 10^{-10} to 10^{-9} per nucleotide base pair per cell division (*2*), perhaps as low as possible given reasonable energy constraints. What about selection—can it be suppressed? There are population structures where this is the case, such as when a large population of differentiated cells is continuously renewed by the asymmetric division of stem cells (*3*, *4*). It has been hypothesized that many epithelial tissues, which are especially susceptible to cancer because of their many cell divisions, are designed to suppress selection (*3*). Intestinal epithelium is replenished by equipotent stem cells residing at the bottom of crypts. These stem cells are continuously replacing each other in a random fashion (*5*, *6*). Most intestinal tumors are thought to initiate from a transformed (mutated) stem cell, because genomic alterations occurring in differentiated cells would be "flushed out" as a result of the specific tissue architecture (differentiated cells are continuously pushed upward in the crypt and eventually undergo programmed cell death at the top of the crypt) (*3*, *7*). The initiating genetic event in the majority of colorectal cancers is an inactivation of the *APC* tumor suppressor gene, often followed by mutations in the oncogene *KRAS* and the tumor suppressor *P53*, among other genes (*8*).

To measure the effect of initial genetic changes occurring in colorectal cancer, Vermeulen *et al*. visualized and quantified the dynamics of stem cell replacement in the mouse intestine when one of the stem cells in the crypt contains a particular change, such as an inactivation of one or both copies of *Apc*, activation of *Kras*, or a mutation in *p53*. The authors demonstrate that the evolutionary dynamics of stem cells can be well described by a simple mathematical model that assumes a ring of five to seven stem cells at the base of the crypt. A mutant stem cell replaces its neighboring wild-type stem cell with probability P_R, whereas the wild-type cell replaces the mutant with probability $1 - P_R$ (see the figure).

Vermeulen *et al*. show that *Apc* inactivation and *Kras* activation increase the probability that a stem cell carrying those alterations replaces a neighboring wild-type stem cell. It is generally believed that inactivation of one of the *Apc* alleles does not lead to a phenotypic change, but the authors found that *Apc* exhibits some degree of haploinsufficiency (*9*): Even a single inactivated *Apc* copy ($Apc^{+/-}$) leads to some selective advantage over wild-type stem cells. The probability that an $Apc^{+/-}$ mutant cell replaces an $Apc^{+/+}$ wild-type cell is estimated to be $P_R = 0.62$. Stem cells with both copies of *Apc* inactivated, $Apc^{-/-}$, replaced neighboring $Apc^{+/-}$ cells with probability $P_R = 0.69$. Activation of *Kras* had

[1]Program for Evolutionary Dynamics, Harvard University, Cambridge, MA 02138, USA. [2]Department of Mathematics, Harvard University, Cambridge, MA 02138, USA. [3]Department of Organismic and Evolutionary Biology, Harvard University, Cambridge, MA 02138, USA. E-mail: martin_nowak@harvard.edu

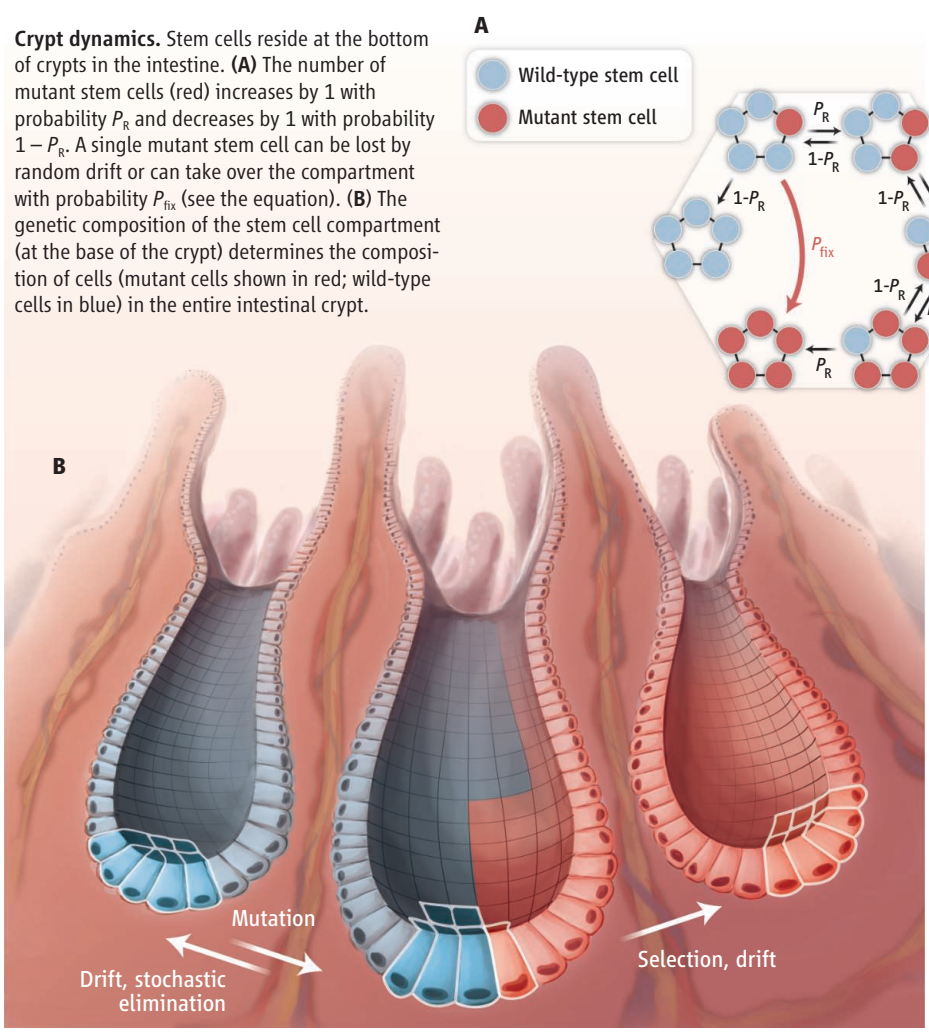

Crypt dynamics. Stem cells reside at the bottom of crypts in the intestine. **(A)** The number of mutant stem cells (red) increases by 1 with probability P_R and decreases by 1 with probability $1 - P_R$. A single mutant stem cell can be lost by random drift or can take over the compartment with probability P_{fix} (see the equation). **(B)** The genetic composition of the stem cell compartment (at the base of the crypt) determines the composition of cells (mutant cells shown in red; wild-type cells in blue) in the entire intestinal crypt.

CREDIT: V. ALTOUNIAN/*SCIENCE*

Published by AAAS

the most pronounced effect, with a 78% chance of replacing an adjacent wild-type stem cell. The authors also found that *p53* mutations provide a selective advantage, but only in gut affected by inflammation (P_R = 0.58) and not in normal conditions (P_R = 0.48).

Although mutant stem cells are more likely to replace wild-type stem cells than vice versa, they can nevertheless be lost by random drift (when the frequency of mutant cell in a population decreases until it disappears). The probability that a single mutant stem cell reaches fixation in a crypt (takes over the entire stem cell compartment of the crypt) can be calculated as

$$P_{\text{fix}} = \frac{1 - \left(\frac{1 - P_R}{P_R}\right)}{1 - \left(\frac{1 - P_R}{P_R}\right)^N}$$

in which N is the number of stem cells per crypt. Assuming $N = 5$ stem cells in a crypt and using the experimentally derived values for P_R, the probability for a single $Apc^{+/-}$ stem cell to take over the crypt is 0.42. Similarly, the probability that a single $Apc^{-/-}$ cell reaches fixation in an $Apc^{+/-}$ background is 0.56. The authors report similar fixation probabilities based on direct measurement.

This detailed quantitative information about the initial steps in the somatic evolution of a solid cancer makes an important connection between theory and experiment. The values for the selective advantage of frequently occurring mutations can provide precise guidelines for future studies of tumor initiation and progression (*10*–*15*). As Vermeulen *et al*. point out, a similar approach can be used to investigate the role of chromosomal instability in tumor initiation. Their findings also raise new questions about the events that follow the fixation of a mutation in a single crypt, including quantification of a field cancerization effect and the change in dynamics and tissue morphology caused by the subsequent mutations. Most important, this exciting study opens the door for a quantitative understanding of cancer initiation. One can also envisage the possibility of using the devised experimental framework for the development and testing of drugs that attack mutated stem cells, thereby preventing the process of cancer initiation.

References

1. L. Vermeulen *et al*., *Science* **342**, 995 (2013).
2. D. J. Araten *et al*., *Cancer Res.* **65**, 8111 (2005).
3. M. A. Nowak, F. Michor, Y. Iwasa, *Proc. Natl. Acad. Sci. U.S.A.* **100**, 14966 (2003).
4. E. Lieberman *et al*., *Nature* **433**, 312 (2005).
5. C. Lopez-Garcia, A. M. Klein, B. D. Simons, D. J. Winton, *Science* **330**, 822 (2010).
6. H. J. Snippert *et al*., *Cell* **143**, 134 (2010).
7. N. Barker *et al*., *Nature* **457**, 608 (2009).
8. S. Jones *et al*., *Proc. Natl. Acad. Sci. U.S.A.* **105**, 4283 (2008).
9. N. L. Solimini *et al*., *Science* **337**, 104 (2012).
10. R. Meza, J. Jeon, S. H. Moolgavkar, E. G. Luebeck, *Proc. Natl. Acad. Sci. U.S.A.* **105**, 16284 (2008).
11. I. Bozic *et al*., *Proc. Natl. Acad. Sci. U.S.A.* **107**, 18545 (2010).
12. R. Durrett *et al*., *Theor. Popul. Biol.* **78**, 54 (2010).
13. C. Tomasetti, B. Vogelstein, G. Parmigiani, *Proc. Natl. Acad. Sci. U.S.A.* **110**, 1999 (2013).
14. B. Vogelstein *et al*., *Science* **339**, 1546 (2013).
15. D. Wodarz, N. L. Komarova, *Computational Biology of Cancer: Lecture Notes and Mathematical Modeling* (World Scientific, Hackensack, NJ, 2008).

10.1126/science.1247887

MATERIALS SCIENCE

Metamaterials Beyond Optics

The area of metamaterials may expand to find application in mechanics, acoustics, and thermodynamics.

Martin Wegener

So far, the field of metamaterials has largely dealt with negative refractive indices in optics and invisibility cloaks (*1*–*3*). However, the underlying idea of designing material properties is not that narrow. More broadly, one rationally designs a subwavelength unit cell from existing constituent materials and (periodically) arranges it into an artificial solid. The properties of that solid are then determined by structure rather than chemistry and can be tailored, extreme, or even qualitatively unprecedented. Rational design is the key and makes metamaterials a rather particular class of composite materials.

In terms of application, some aspects of metamaterials such as negative phase velocities of light (*1*, *2*), invisibility cloaking (*4*, *5*), or unusual optical nonlinearities (*6*) are fascinating but are not likely to soon appear in products, because optical absorption (loss) is too high and in part fundamentally unavoidable. Moreover, the inexpensive manufacturing of complex large-volume three-dimensional optical metamaterials is still a formidable challenge in itself (*2*).

Why, then, don't we go beyond optics and also consider other material aspects (*7*) such as thermal, acoustic, elastic, or irreversible nonlinear mechanical properties? The corresponding wavelengths and length scales range from tens of micrometers to centimeters, rather than nanometers in optics. Hence, fabrication limitations are relaxed, thus easing real-world applications. Moreover, one lesson learned from electromagnetism is that off-resonant constituents enable low losses. In the visible spectrum, however, this results in a contrast in refractive index of no more than 3 for available nonabsorbing dielectrics. Some theoretical blueprints demand constituent-material contrasts in the range of tens or hundreds. Such values are accessible in mechanics and thermodynamics (see the figure).

Consider simple mechanical waves in elastic solids. They exhibit three orthogonal polarizations, one longitudinal (like sound waves in air or water) and two transverse (like electromagnetic waves). This complex

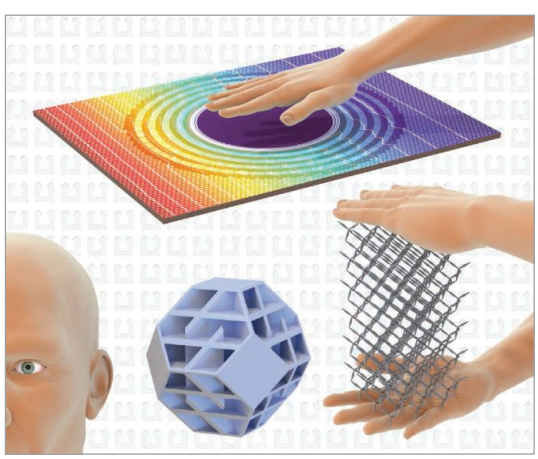

Seeing, hearing, feeling. While optics has been in the foreground of metamaterials research, opportunities arise in other areas such as acoustics, mechanics, and thermodynamics (heat conduction and diffusion). In all of these, larger lattice constants ease the fabrication requirements and losses can be much lower or absent.

CREDIT: ROBERT SCHITTNY, KARLSRUHE INSTITUTE OF TECHNOLOGY

Institute of Applied Physics, Institute of Nanotechnology, and DFG Center for Functional Nanostructures, Karlsruhe Institute of Technology, D-76131 Karlsruhe, Germany. E-mail: martin.wegener@kit.edu

Published by AAAS